ELSEVIER

Journal of Chromatography A, 855 (1999) 367–382

JOURNAL OF CHROMATOGRAPHY A

www.elsevier.com/locate/chroma

Visualization of sample introduction in liquid chromatography columns
The effect of the frit diameter

B. Scott Broyles[a,b], R. Andrew Shalliker[a,b,1], Georges Guiochon[a,b,*]

[a]*Department of Chemistry, The University of Tennessee, Knoxville, TN 37996-1600, USA*

[b]*Chemical and Analytical Sciences Division, Oak Ridge National Laboratory, Oak Ridge, TN 37831-6120, USA*

Received 25 May 1999; received in revised form 11 June 1999; accepted 11 June 1999

Abstract

A previously developed on-column detection technique using 35 mm SLR cameras [*J. Chromatogr. A* 826 (1998) 1] was employed to visualize colored sample bands as they elute through frits of differing diameter. Head fittings containing a 4.0 mm frit and a 15.9 mm frit were mounted in a 17 mm I.D. glass column packed with C_{18} silica with an average particle size of 21 μm. A carbon tetrachloride mobile phase of matching refractive index to that of the silica provides clarity along the column diameter during band migration. The photographs of the migrating sample zones were scanned and analyzed with appropriate imaging software. The smallest diameter frit induced severely parabolic sample distributions at the column inlet compared to the larger frit. Local axial dispersion coefficient values, expressed as local reduced plate height, were calculated as well as local zone velocities at the column inlet. The results demonstrate clearly the need to match the diameter of the inlet frit to the I.D. of the column so as to avoid the initial onset of zone broadening due to the frit.

Keywords: Frit diameter; Visualization of sample introduction; Sample introduction

1. Introduction

The visualization of bands in chromatographic columns offers the possibility of a detailed examination of the numerous phenomena that may take place during the entire analytical process [1]. It even offers the ability to unravel, at least to a degree, the intricacies of their interactions. Chromatographers often overlook the importance of sample introduction onto the head of the column. In previous studies, we showed the dramatic effects that a leak around the edge of a frit may produce and how a property apparently as minor as the porosity of the frit may influence the shape of the band introduced into the column [2]. Furthermore, the results of this study suggest that frits are radially heterogeneous and poorly reproducible. Variations of permeability from one frit to another having the same nominal porosity may be substantial. Poor sample introduction through a heterogeneous frit may make a column look poorly

*Corresponding author. Tel.: +1-423-974-0733; fax: +1-423-974-2667.

E-mail address: guiochon@utk.edu (G. Guiochon)

[1]Present address: Faculty of Science and Technology, University of Western Sydney, Hawkesbury, Richmond, New South Wales, Australia.

0021-9673/99/$ – see front matter
PII: S0021-9673(99)00737-2

packed, when in reality its bed is behaving efficiently and uniformly [2].

Central sample introduction was shown to increase the column efficiency [3]. This, however, requires that the sample be injected directly onto the packing [1,3] – and the practicality of this approach is limited. Otherwise, if a sample centrally injected impinges directly onto an inlet frit located on top of the packing, migration of the sample does not proceed in the manner of the 'infinite diameter' column despite its central location [1]. Efficiency measurements have shown that this expected behavior is not observed [1], due to the establishment of unequal flow profiles resulting from the mobile phase dispersing radially towards the wall, at the frit. This radial flow of the mobile phase carries with it part of the sample band and, consequently, the sample is distributed unevenly across the column head. The column efficiency suffers as a result. Consequently, sample introduction that is uniformly distributed across the top of the column from the outset is preferred.

In recent years there has been a growing trend toward the development of encased frits, i.e., of frits that are encased within a polymer collar [typically, stainless steel may be encased within a polyether ether ketone (PEEK) ring]. It is important that chromatographers use the correct fitting that matches their column. A quick scan through manufacturer catalogues (e.g. Refs. [4–6]) reveals a variety of models of encased frits. The user may choose between different materials (e.g. for biocompatibility), pore sizes, outside case diameters or diameters of the internal frit component. Many of these frits are designed for pre-column filters or pre-injection filters and are not intended for use within a column head fitting. In some instances, the information is not explicit, with one manufacturer advising the selection of a narrow internal frit diameter for slow flow-rates and of wider frits for higher flow-rates. Finally, most of these frits fit perfectly into a standard analytical column head piece (1/4 in. O.D.; 1 in.=2.54 cm). However, there are now other common standards. Visually, a 4.6 mm I.D. column is hard to tell from a 4.1 mm I.D. one, which, in turn, is visually indistinguishable from a 3.9 mm I.D. column. Because chromatography is so widely used in the chemical industry and the main concern of analysts is the rapid performance of a certain separation, it is not surprising that errors in the frit choice could be frequent.

The exact advantages of an encased frit have not been well documented. We assume that the polymer ring, which should lie exactly atop of the column wall – no thicker and no thinner, prevents the fluid flow from reaching the outer edges of a standard one piece frit that fits inside the head piece, thereby minimizing any back flow within the frit itself. Presumably this improves the efficiency. This could also avoid that the mobile phase flow bypasses the frit, with deleterious effects on column efficiency and separation ability [1]. An incorrect choice with regards to the frit diameter may have a drastic effect on the column performance [7], but to date very little work has been carried out to evaluate this effect.

In this work, we present a systematic illustration of how the frit diameter affects the efficiency of the column. To do so, we employed a visualization technique involving the use of glass column tubings and of matched mobile and stationary phases that have the same refractive indices. In such a situation the bed is entirely transparent. Consequently, if a colored sample is injected onto the column, its migration can be monitored during its entire elution. We used this technique on several occasions to observe viscous fingering [8], solute migration [1,7] and to evaluate the effect of frit porosity [2].

2. Experimental

The chemicals, reagents, equipment and data analysis procedures used for the visualization of chromatographic bands were described in previous communications [1,7,9]. The only new information of importance to this study involves the design of the column head fitting.

The inlet assembly is shown in Fig. 1. It consists of the variable inlet head that contains the inlet frit. The diameter of the inlet frit was changed systematically in relation to the column internal diameter. Frits with diameters of 4.9 mm, 13 mm and 15.9 mm were examined (we could not find a frit of external diameter matching exactly the column used (I.D., 17 mm). All pore sizes were either 2 μm or 10 μm, as stated in the text when relevant. This

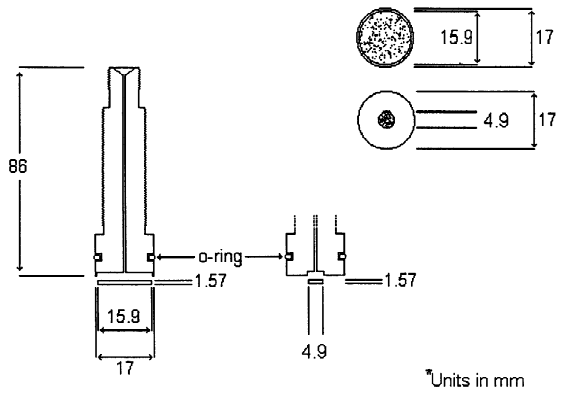

Fig. 1. Diagram of the column header containing the frit.

assembly was then inserted into the glass column. The head was tightened to a torque of 0.2 m·kg. The column was then allowed to sit overnight before testing. Because of the column design, the inlet assembly could not be removed without perturbing significantly the bed around the column inlet or even the possibility of destroying the packed bed. As a result, it was necessary to pack a new column for each of the different configurations tested. All injection volumes were 20 μl.

3. Results and discussion

In a previous work, we showed the importance of the porosity of the frit in controlling the radial uniformity of the sample band [2]. In general, for columns packed with 20–30 μm particles and for frits with diameters close to the column internal diameter, a more uniform flow profile was established with an average frit pore size of 10 μm than with a size of 2 μm. The sample that entered through the 2 μm frit had a slightly parabolic shape, resulting in a radial variation of the migration rate of the sample and in a poor column efficiency, with peak tailing.

If there is flow restriction at the inlet of the column because the inlet frit employed is narrower than the column and allows solute access into the column only in the central region, the migration profile is very different from the expected planar profile used in theoretical models. This is illustrated by the series of photographs in Fig. 2. Fig. 2a shows the sample zone as it just enters the column. Further migration shows that instead of the sample remaining in the central region of the column, the band projects radially, pushing the sample radially towards the wall and dispersing it in the process (Fig. 2b). Finally, after the leading edge of the sample has migrated ca. 21.9 mm along the column in the axial direction, the tailing edge of the sample reaches the wall (Fig. 2c). The axial symmetry of the band profile is shown in Fig. 2d. As a result of the initial entry of the band into the central region of the column, the overall column efficiency is very poor. This can be graphically illustrated by evaluating sample migration profiles along individual flow streams.

The process for extracting these profiles has previously been discussed and need not receive further comment [9]. Fig. 3a illustrates the concentration profiles for column slices parallel to the camera and the column axis on the left-hand side (LHS) of the column and Fig. 3b illustrates the same concentration profiles for the right-hand side (RHS) of the column. Clearly, there is a large radial variation of the mobile phase velocity across the sample band (the solute used, iodine, is not significantly retained under the experimental conditions). The band profile resulting from this distribution of the flow velocity across the column inlet changed little along the entire column length as the migration profiles in Figs. 4a (LHS) and 4b (RHS) illustrate. These profiles were obtained after the sample had migrated approximately 50 mm along the column.

A plot of the local efficiency versus the column radius is shown in Fig. 5. Curve (a) represents the efficiency obtained from the profiles in Fig. 3, while the efficiency values in curve (b) were obtained from the profiles in Fig. 4 (migration distances, ca. 22 and 72 mm, respectively). The efficiency of this column is apparently very poor (average $h=8.9$, derived from the peak second moments), especially near the wall region (where $h=21.1$ for LHS, $h=17.2$ for RHS). The overall migration profile obtained by summing the individual profiles in Fig. 4 gives a reduced plate height value of 17.9. This accounts both for axial dispersion and for the consequences of the radial inhomogeneity of the injection profile. The zone broadening contributions of the tailing flow

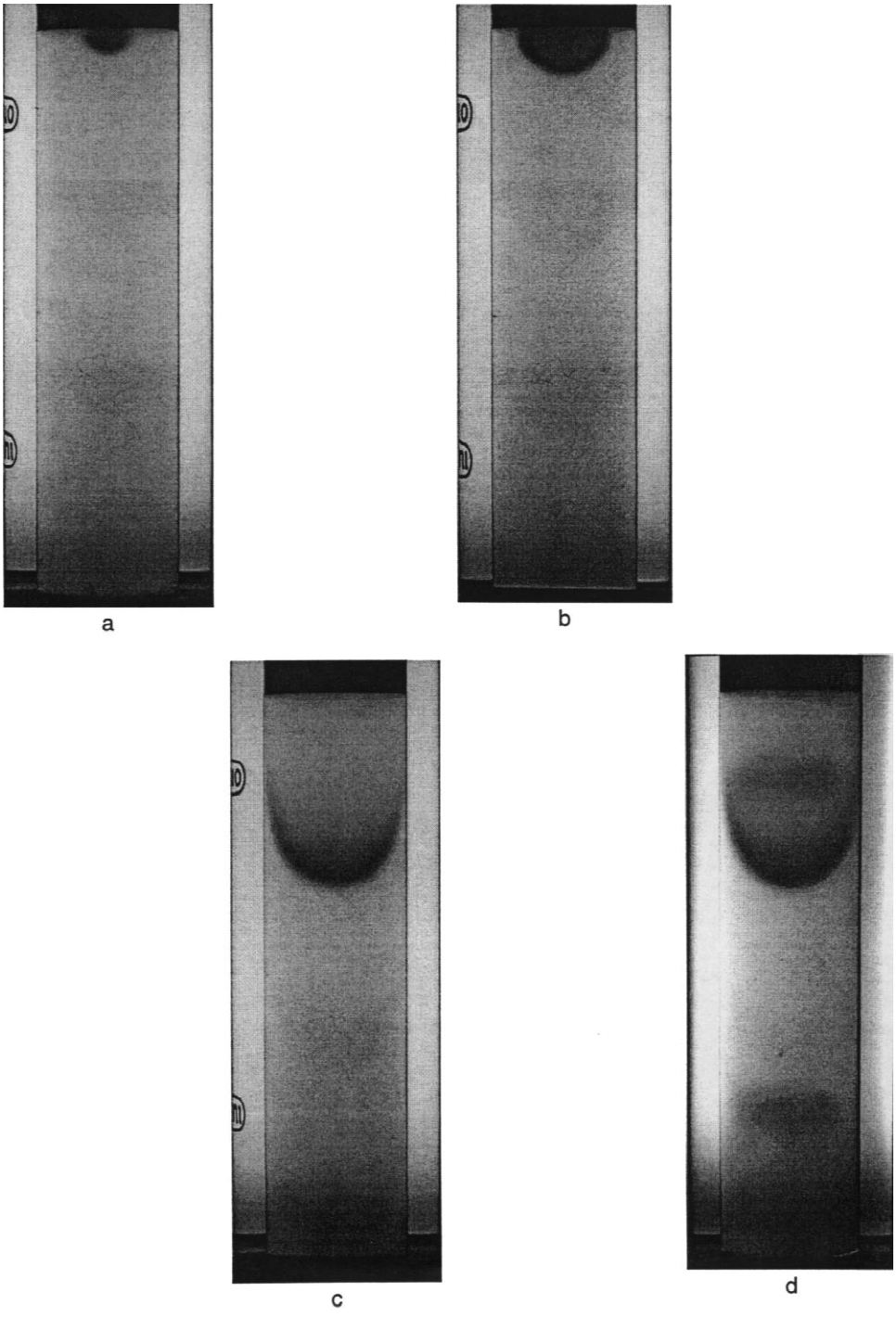

Fig. 2. Photographs of a band of iodine entering a column fitted with a 10 μm narrow frit. (a), (b) And (c) photographed from camera 1. (d) Photographed from camera 2, at right angle to camera 1. Flow rate=1.5 ml min^{-1}.

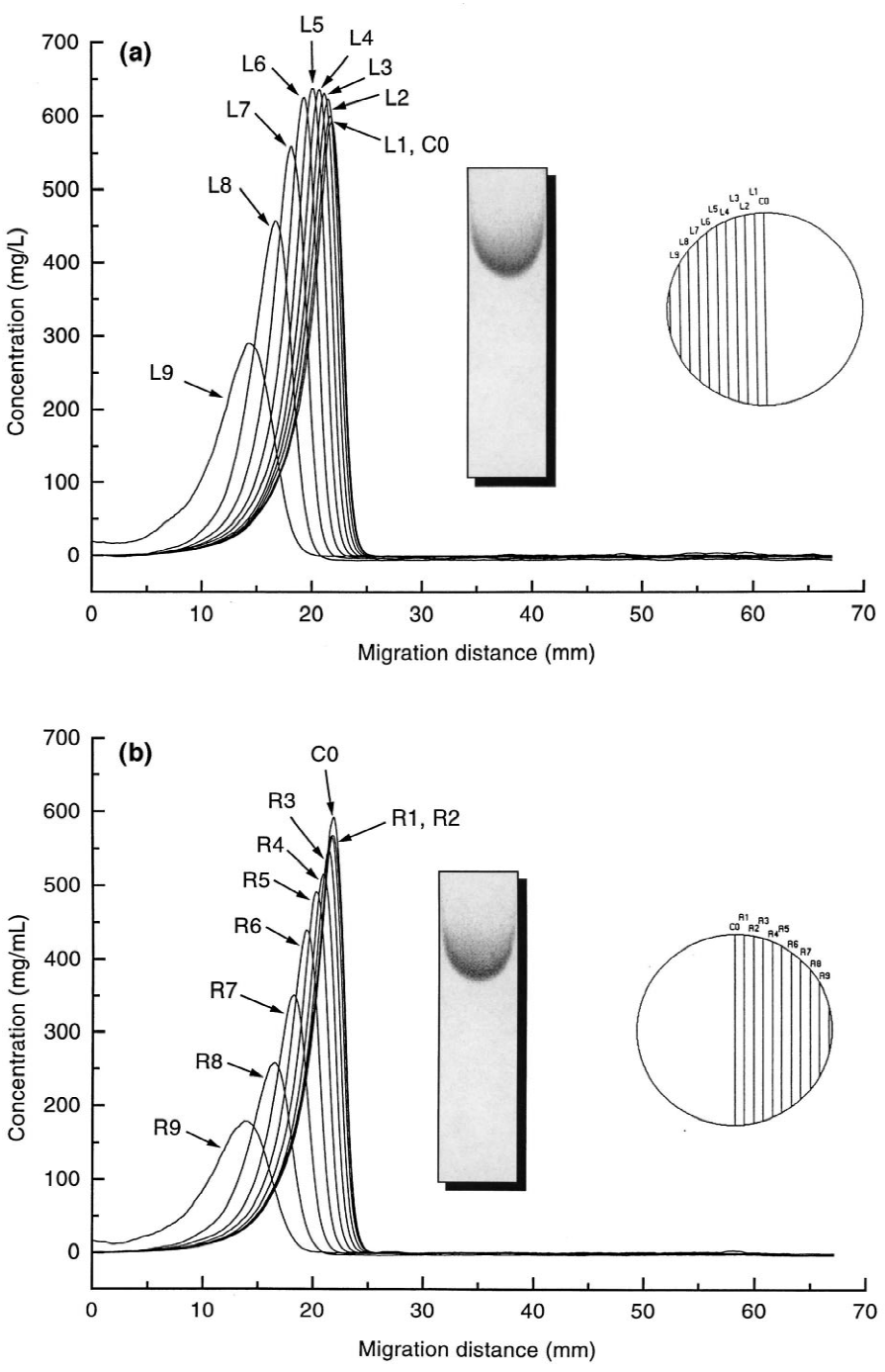

Fig. 3. Axial concentration profiles obtained by scanning the vertical bands (whose horizontal traces are shown in the right inset) of the image in the left inset, obtained with camera 1, 2 min after sample injection on a column with a 4.9 mm diameter 10 μm frit. The photograph was taken under the same conditions as Figs. 2a and b. Each band is 0.81 mm wide (approximately 40 particle diameters). The image was divided into 19 sections radially across the column, as indicated in the right inset. (a) Profiles for the left hand side of the column including the center. (b) Profiles for the right hand side of the column including the center.

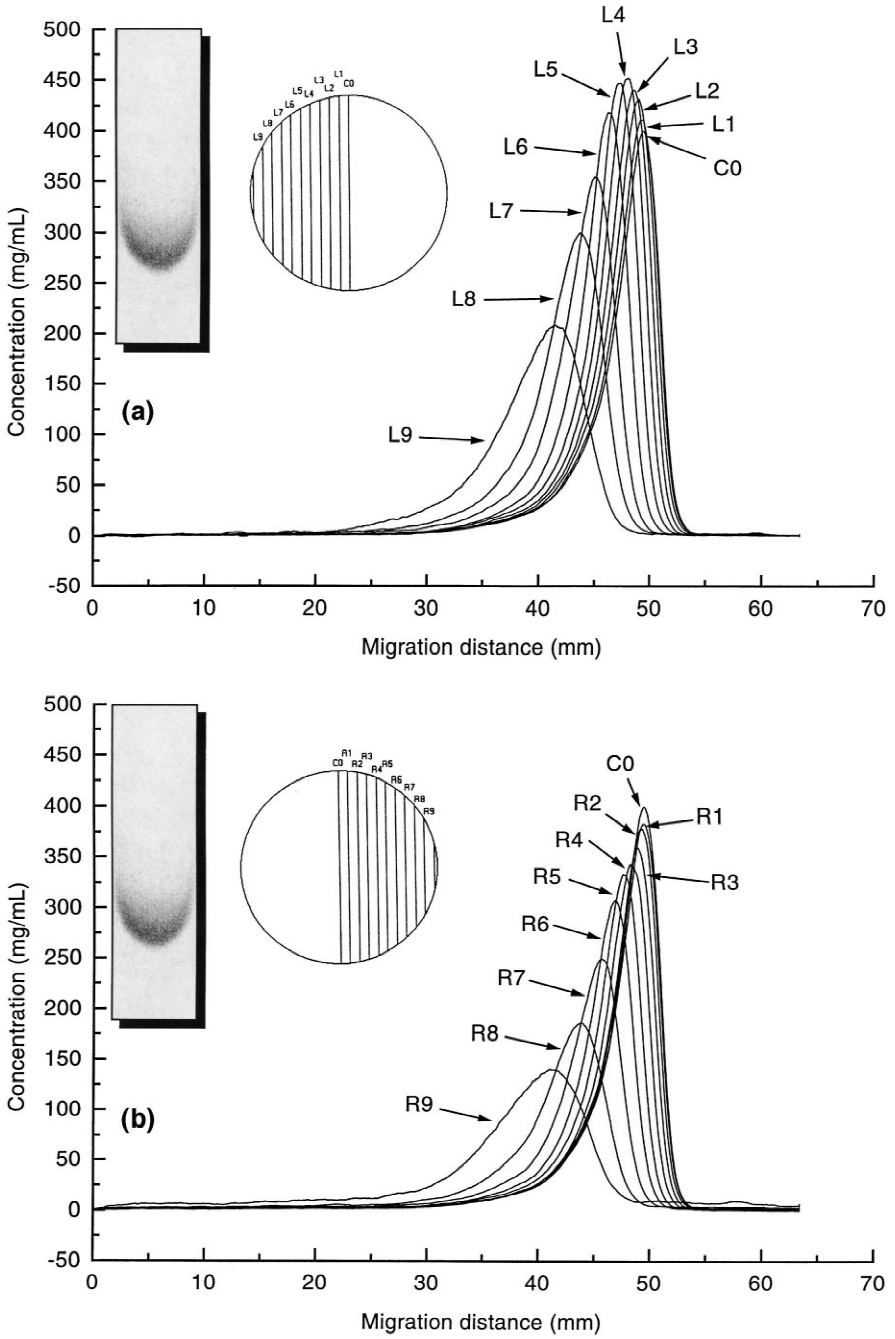

Fig. 4. Axial concentration profiles obtained by scanning the vertical bands (whose horizontal traces are shown in the right inset) of the image in the left inset, obtained with camera 1, 5 min after sample injection on the column in Fig. 3. Each band is 0.81 mm wide (approximately 40 particle diameters). The image was divided into 19 sections radially across the column, as indicated in the right inset. (a) Profiles for the left hand side of the column including the center. (b) Profiles for the right hand side of the column including the center.

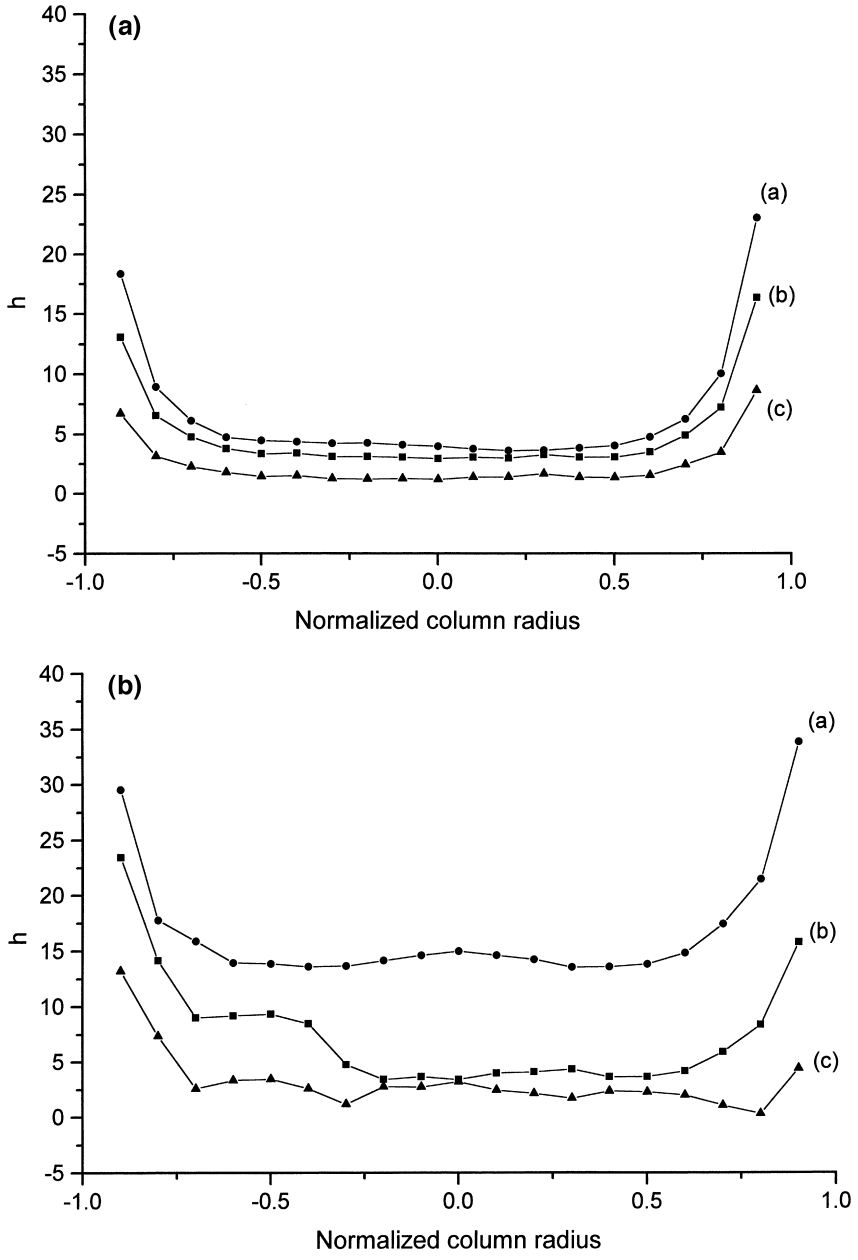

Fig. 5. Plot of the reduced plate height versus the radial location. (a) For profiles shown in Fig. 3. (b) For profiles shown in Fig. 4. (c) For the bed section between the profiles in Fig. 3 and Fig. 4. (a) h Calculated using the peak width at half height. (b) h Calculated using the peak second moment.

streams has reduced the column performance significantly. However, the central region of the column is reasonably uniform. In this case, the 'wall effect' is not to be blamed for the poor column performance. Subtraction of the early band variance from the later band variance allows the derivation of the contribution of the column bed itself. The true bed efficiency is shown in Fig. 5, curve (c). Clearly, the

bed behaves more efficiently than observation of the profiles would have predicted. The poor column performance arises from the unsuitable profile of the streampath of the mobile phase flow at column inlet. Once established (Fig. 2c), the profile merely travels along the column with a slow axial dispersion.

An estimate of the distribution of the mobile phase velocity near the head of the column was obtained from a long series of photographs. They were taken first at 4-s intervals, for 56 s; then a photograph was taken at 1 min intervals up to the time the band reached the outlet frit. The four photographs shown in Fig. 2 belong to this series. Fig. 6 shows the grayscale intensity profiles for the axial scans made along the column axis for each photograph. Conversion from grayscale intensity to concentration is not necessary since we need only the peak maxima to derive the migration distance of the band at the corresponding time. Radial scans made at the head of the column, in the direction perpendicular to the column axis are shown in Fig. 7. These profiles are not symmetrical about the column axis, indicating a heterogeneous distribution of sample concentration induced by the frit. The left-hand side of these profiles were used to determine the migration distance in the radial direction since distortions prevalent on the right-hand side made determination of the local peak maxima difficult. Plots of the migration distance vs. time for both the axial and the radial displacement are shown in Fig. 8.

Fig. 8a depicts the displacement of the band in the axial direction. It shows two distinct regions of linear behavior. Best fit lines were determined for each linear region; the linear velocity is represented by the slope of the line. The first region extends down the column bed for approximately the first 5 mm and the corresponding linear velocity is 0.347 mm s^{-1}. However, at the inlet, the frit is narrower than the column, so, the flow velocity is higher. Progressing along the column, the streamlines diverge around the particles of the packing material and the linear velocity of the mobile phase decreases. As a result, in the second region of the column, the average velocity decreases to 0.155 mm s^{-1}, less than half its initial value. Fig. 8b shows the radial displacement of the sample vs. time. In a somewhat arbitrary fashion, three velocity regions can be distinguished and the radial mobile-phase velocity determined in

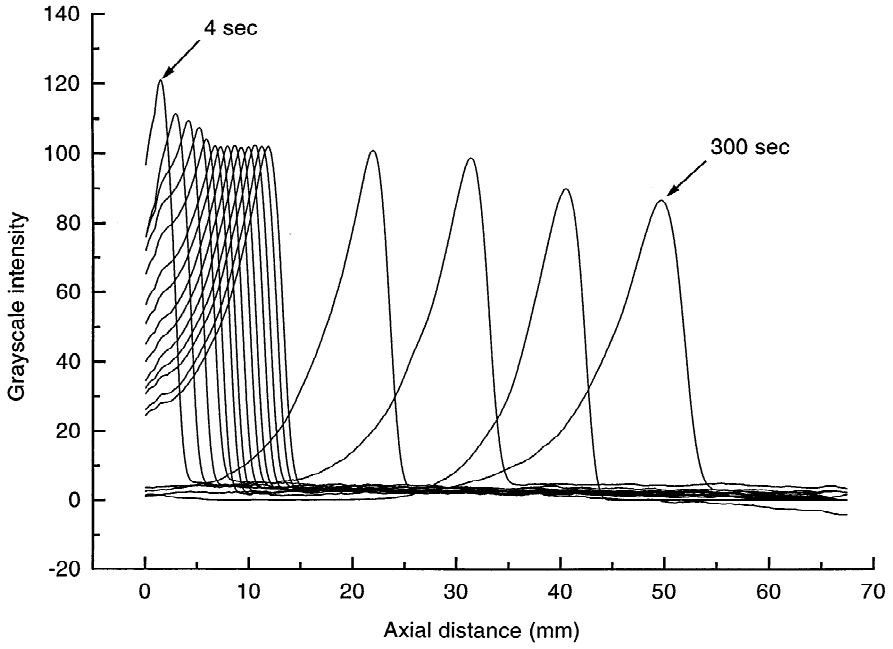

Fig. 6. Axial grayscale intensity profiles obtained by scanning at the column center with a 0.81 mm wide (approximately 40 particle diameters) scan line.

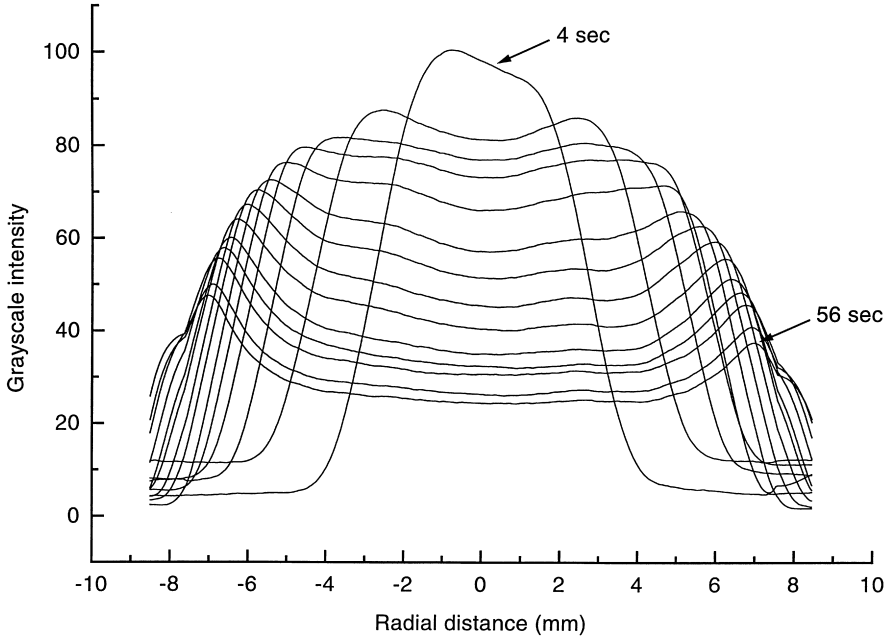

Fig. 7. Radial grayscale intensity profiles obtained by scanning at the top of the column just below the frit with a 0.81 mm wide (approximately 40 particle diameters) scan line.

each of them. A best fit straight line was fitted to the data points in each region, with the slope representing a reasonable estimate of the local mobile-phase velocity. The first region ranges from 0 to 4.0 mm and exhibits a high velocity of 0.38 mm s^{-1}, comparable in magnitude to the velocity in the axial direction, during about the same time period. In the second region, ranging from 4.5 to 6 mm, the average velocity is around 0.10 mm s^{-1}. In the third region, ranging from 6 to 8.5 mm, or terminal velocity region, the radial velocity (average in this region, 0.040 mm s^{-1}) drops to zero as the sample zone approaches the column wall.

Not only was the flow velocity poorly distributed, but the sample concentration across the column was also poor. Examination of the peak areas (cf. Figs. 3a and b) normalized to the area of the profile in the column center (Fig. 9) clearly shows that the solute concentration in the LHS of the column is higher than in the center and in the RHS. This observation suggests that the unsymmetrical nature of the concentration distribution is explained by the lack of homogeneity of the frit which has a higher permeability on the LHS compared to the RHS. Such a result was not previously reported but we suspect that it is general. However, because the frit was narrow, no irregularities in flow symmetry were discernable even through close inspection of the dual aspect photographs. The consistency in the concentration distribution throughout the length of the column clearly indicated that the frit was to blame and not the bed itself.

To further evaluate whether possible frit irregularities may have contributed to the flow profile, we injected a sample of iodine onto the column through the same head piece containing only a glass fiber filter sheet covering the 1/16 in. inlet hole. This column could not be compressed due to the limitations originating from the use of a glass fiber filter. However, the phenomena associated with the sample introduction were quite similar to those observed with the inlet frit described above.

No 10 μm frits of intermediate diameter were available for testing. However, injections were made with a 2 μm frit which had a diameter (13 mm) intermediate between that of a large frit covering nearly all the column cross-section (diameter 15.9 mm, see later) and that of the narrow frit discussed

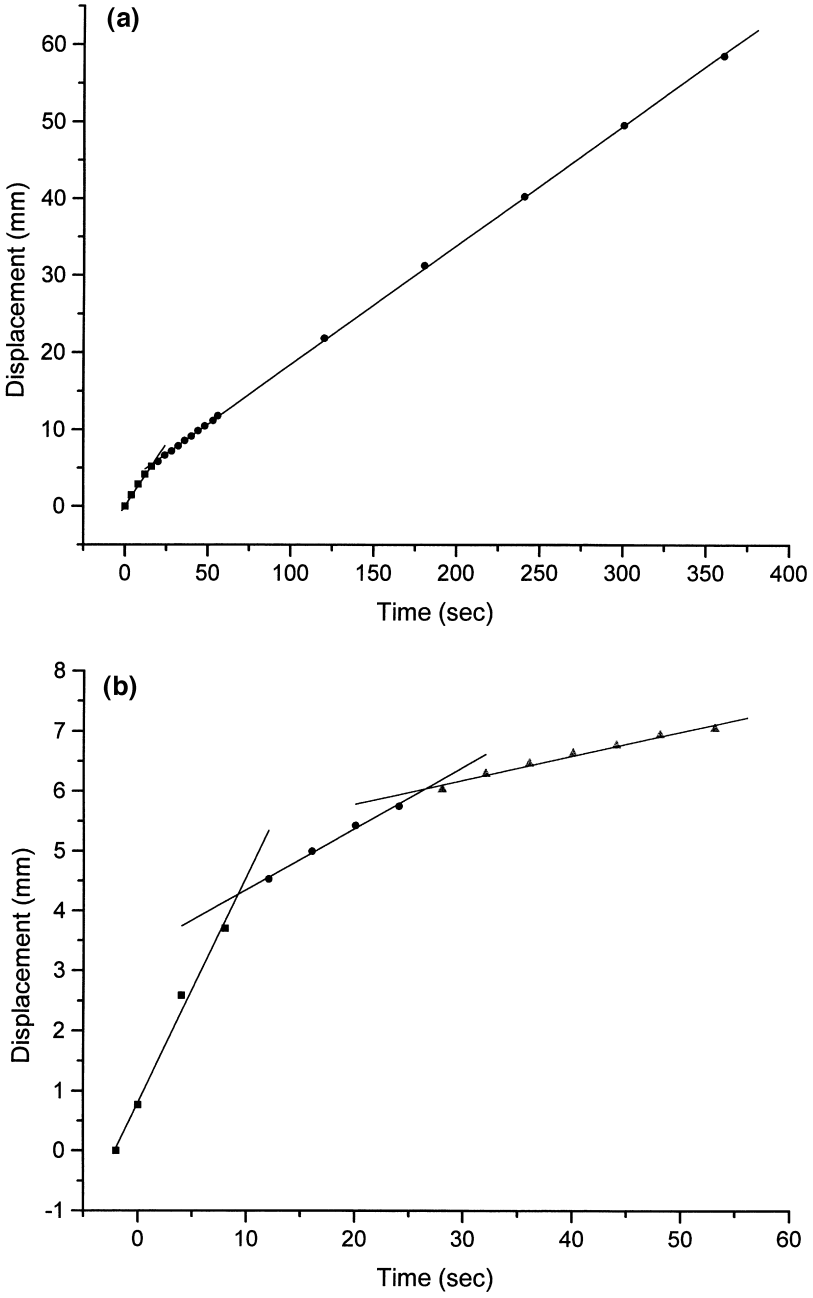

Fig. 8. Plots of migration distance (taken as peak maxima) versus time for axial and radial grayscale intensity profiles. (a) For axial scans in Fig. 6. (b) For radial scans in Fig. 7.

earlier (4.9 mm, Fig. 2). The results observed were explained by a simple decrease of the extent of the distribution zone located at the column inlet. Fig. 10 shows typical profiles representative of those obtained upon injections made on frits of this diameter and porosity. The evaluation of the peak profiles and

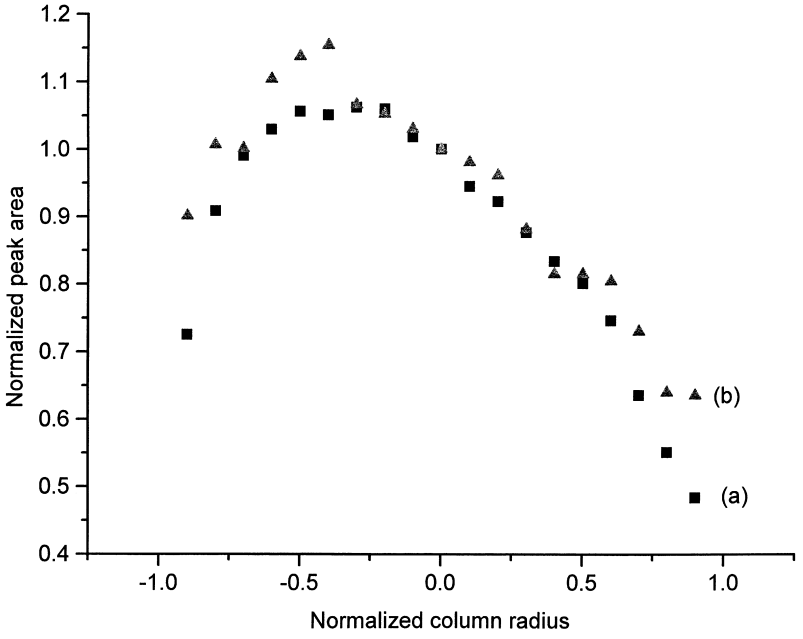

Fig. 9. Plot of the area under each concentration profile normalized to the area of the central band profile, versus the column radius. The area under the central band profile is taken as unity. (a) Areas for the profiles in Fig. 3. (b) Areas for the profiles in Fig. 4.

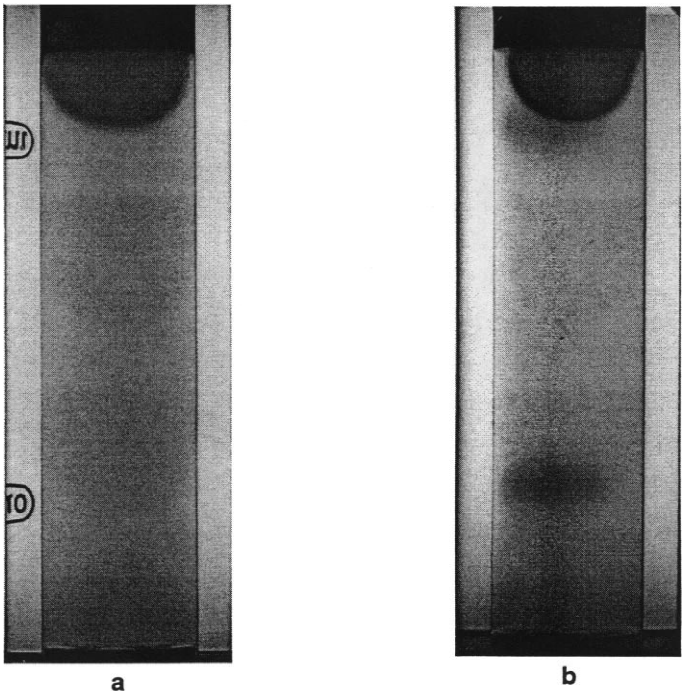

Fig. 10. Photographs of a band of iodine entering a column fitted with a 2 μm intermediate sized (13 mm diameter) frit. (a) Photographed from camera 1. (b) Photographed from camera 2, at right angle to camera 1. Flow rate=1.5 ml min^{-1}.

the radial migration distributions made following the procedures described earlier and illustrated in Figs. 3 to 9 showed results intermediate between those obtained with the narrow frits and those given by wide frits. However, the sample distribution at the head of the column was found to depend both on the

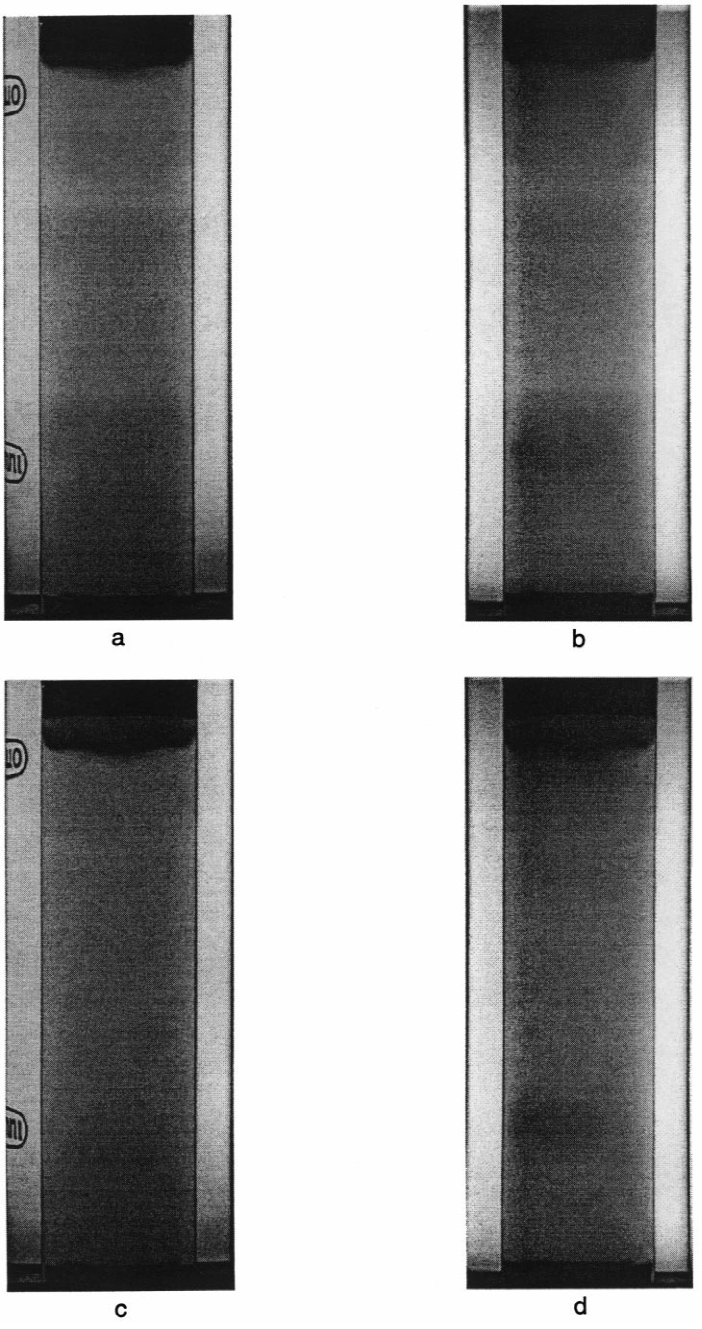

Fig. 11. Photographs of a band of iodine entering a column fitted with a 10 μm wide (15.9 mm diameter) frit. (a) And (c) photographed from camera 1. (b) And (d) photographed from camera 2, at right angle to camera 1. Flow rate=1.5 ml min^{-1}.

frit diameter and on its porosity [2]. Thus, a detailed investigation of the 2 μm frit is not appropriate for comparison with the narrow and wide 10 μm frits and therefore will not be presented here.

We observed a clear trend toward a reduction of the importance of the distribution zone at the head of the column and of the amplitude of the radial variation of the mobile phase velocity when the frit diameter increases. Extrapolating this trend leads to the obvious conclusion that a frit having the same diameter as the column would distribute the sample optimally. Indeed, to some extent, this is the case. Examination of the results obtained with the widest 10-μm-porosity frits (15.9 mm) available for the test columns shows a reduction in the severity of the distribution profiles instigated by the narrower frits. Fig. 11a–d show the injection of the sample zone at 1.5 ml min^{-1}. The photographs taken at the second camera angle (Fig. 11b and d) and corresponding to Fig. 11a and c, respectively, verify zone symmetry. Fig. 12 shows the concentration profiles measured along the individual flow streams on the LHS (Fig. 12a) and the RHS (Fig. 12b) of the column. A nonintrusive artifact of unknown origin appears prior to the rear of the profile, which is of no consequence in the data evaluation. The artifact occurs only rarely; it does not migrate during the course of the experiment.

The sample zone in this case was not distributed homogeneously across the column but its migration is piston-like, with a constant velocity. The iodine concentration is highest near the column wall. It decreases progressively toward the central region of the column. The peak width in Fig. 12 remains nearly constant while the peak height increases with increasing radial distance. Fig. 13 shows the radial distribution of the local values of the reduced height equivalent to a theoretical plate, HETP (h) calculated from the peak width at half-height, from the concentration profiles in Fig. 12. The uniform distribution of h indicates a very homogeneous column bed, despite a heterogeneous distribution of the sample concentration at the column inlet. The mean value of h was 3.2. The total migration profile obtained by appropriate summation of each profile in Fig. 12 [9] is nearly symmetrical and gives a reduced plate height of 3.3. However, not all wide 10-μm frits that we tested gave such uniform and symmetrical sample distributions. Significant variations, presumably due to a heterogeneous distribution of the permeability of the frit, were the most probable explanation for some unsatisfactory results. More importantly, however, all wide 10-μm frits gave significantly better sample distributions than all the narrow frits. This comparison was discussed elsewhere [2].

The performance of various frits are compared and the importance of always using wide frits illustrated in Fig. 14. While a uniform sample concentration distribution across the column radius is optimal, to avoid local column overloading, a most uniform velocity distribution is necessary to minimize zone broadening and peak tailing. Plots of the local velocity, normalized to the velocity at the column center, versus the normalized column radius illustrate the superiority of the wide 10-μm frits over the narrow frits with regards to the velocity distribution at the column inlet. The narrow 10-μm frit shows a high axial-velocity region in the column center with a decrease in the radial velocity when moving toward the wall. This trend is consistent with the shape of the sample zone entering the column. However, as the zone migrates further along the column, we observe a progressive increase of the velocity close to the wall relative to that at the column center [curves (a), (b) and (c)]. This phenomenon takes place because the exit frit is wide and covers the whole column section. In contrast, the large 10-μm frit provides a uniform distribution of the zone velocity across the column radius, independent of the migration time [curve (d)].

4. Conclusions

Intuitively, chromatographers who prepare their own columns understand that the diameter of the frit should equal that of the inner diameter of the column. However, it is not always possible to achieve this ideal, for example when working with axial compression columns in which the head assembly fits inside the column. A finite amount of solid material is required to provide the necessary sealing between the frit and the column wall. This material should be compressible so as to provide a tight fit and no scratching of the inner wall of the column. Such measures are needed to prevent a back wash of

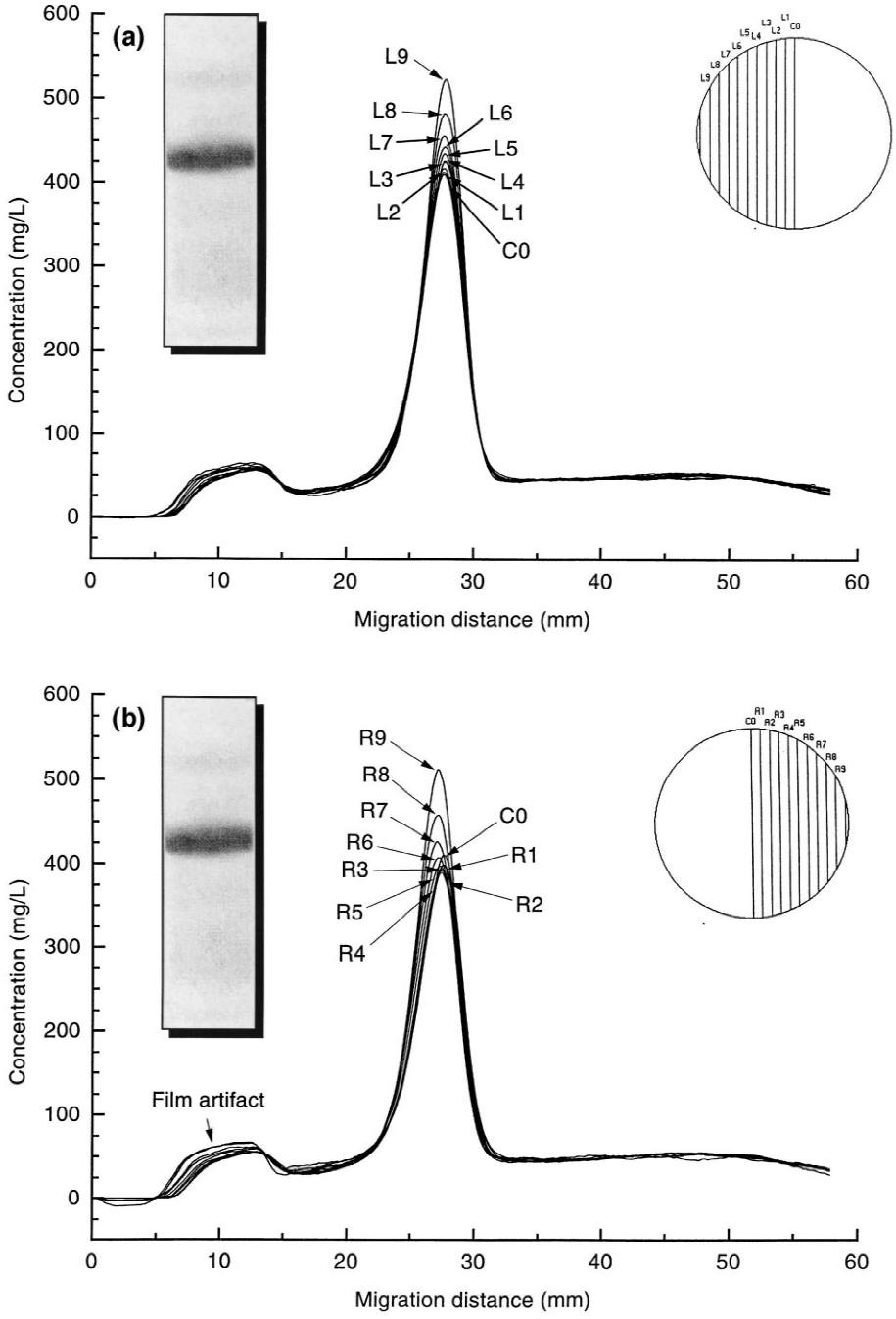

Fig. 12. Axial concentration profiles obtained by scanning the vertical bands of the image in the left inset, obtained with camera 1, 3 min after sample injection on the column. The photograph was taken under the same conditions as Figs. 11a and b. (a) Profiles for the left hand side of the column, including the center. (b) Profiles for the right hand side of the column, including the center.

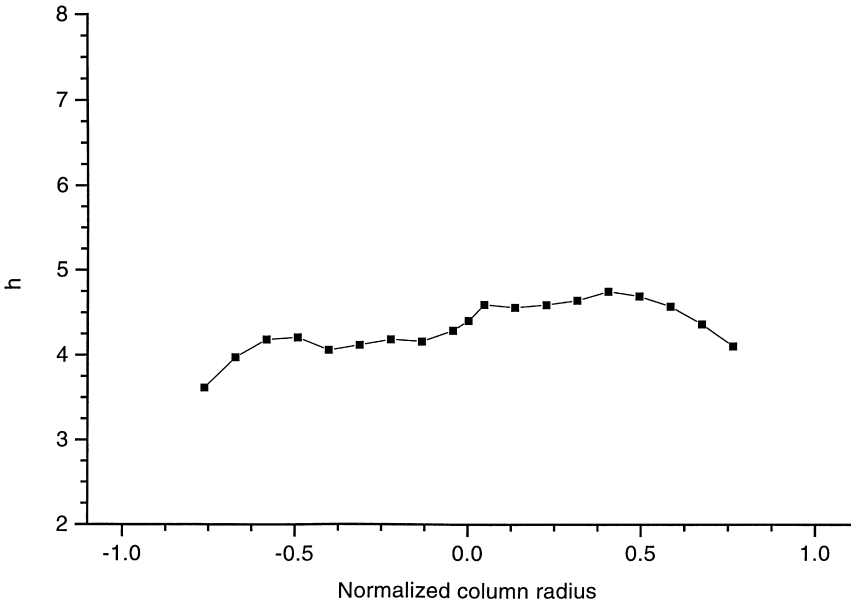

Fig. 13. Plot of the reduced plate height versus the radial location. Column containing the wide 10 μm frit from which the photograph in the inset of Fig. 12 was obtained.

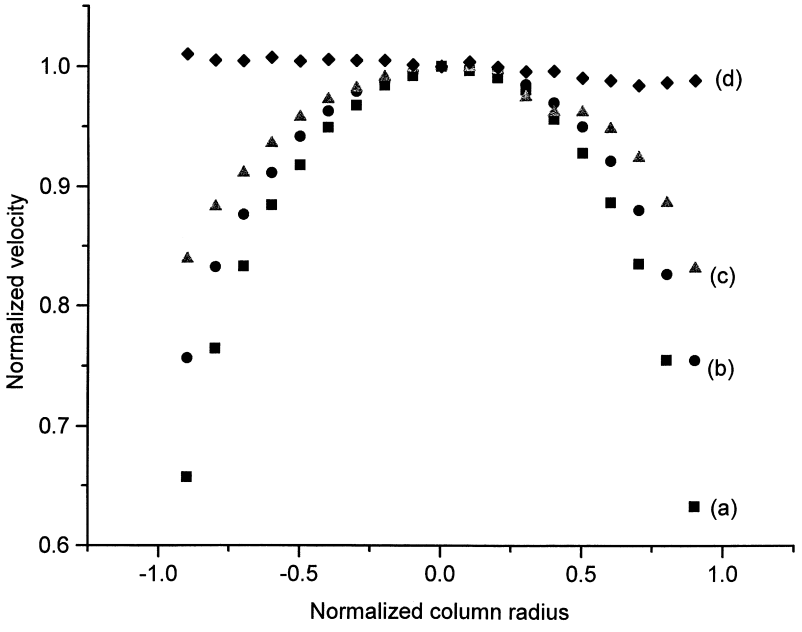

Fig. 14. Plot of the velocities normalized to the velocity of the central band profile, versus the column radius. The velocity of the central band profile is taken as unity. (a) Velocities of the profiles for the narrow 10 μm frit at $t=2$ min (b) $t=3$ min, and (c) $t=5$ min. (d) Velocities of the profiles for the wide 10 μm frit at $t=3$ min.

particles and/or sample around the edges of the frit during column compression and operation. In preparation of such head fittings strict attention must be given to a design that maximizes the frit diameter while still providing the necessary seal at the frit/column interface. As shown, when the frit to column diameter ratio becomes significantly less than unity, severely inhomogeneous flow profiles result. This phenomenon is not unique to a relatively small diameter frit. Large diameter frits with a low porosity can be found to give poor sample distributions similar to, but not as severe as, small diameter frits. These results were presumably due to poor frit homogeneity. However, at no time was a good performing narrow frit found. While the heterogeneity of the frit plays an important role in perturbing the flow profile at the column inlet, this variable cannot be controlled except at the manufacturing level. However, the choice of the frit diameter to use for a particular column diameter is the simplest parameter left in the hands of the chromatographer and column manufacturers.

Acknowledgements

This work was supported in part by Grant DE-FG05-88ER13859 of the US Department of Energy and by the cooperative agreement between the University of Tennessee and the Oak Ridge National Laboratory (ORNL). In addition, we thank Kim Thomas (ORNL) and Mark Barnes (Thompson PhotoStudios, Knoxville) for their assistance in this work.

References

[1] R.A. Shalliker, B.S. Broyles, G. Guiochon, J. Chromatogr. A. 826 (1998) 1.
[2] B.S. Broyles, R.A. Shalliker, G. Guiochon, submitted for publication.
[3] J.J. Kirkland, W.W. Yau, H.J. Stoklosa, C.H. Dilks Jr., J. Chromatogr. Sci. 15 (1977) 303.
[4] 1999 Catalog of Chromatography and Fluid Transfer Fittings, Upchurch Scientific, 1999.
[5] Chromatography Product Guide, Bodman Industries.
[6] Chromatography Catalog 450, Alltech, 1999.
[7] R.A. Shalliker, B.S. Broyles, G. Guiochon, Am. Lab. 30 (21) (1998) 124.
[8] B.S. Broyles, R.A. Shalliker, D.E. Cherrak, G. Guiochon, J. Chromatogr. A. 822 (1998) 173.
[9] B.S. Broyles, R.A. Shalliker, G. Guiochon, submitted for publication.